COMMUNICATION

Double-layered nanoparticle stacks for surface enhanced infrared absorption spectroscopy†‡

Johannes Srajer,‡[ab] Andreas Schwaighofer,‡[a] Georg Ramer,[c] Stefan Rotter,[d] Bilal Guenay,[a] Albert Kriegner,[a] Wolfgang Knoll,[a] Bernhard Lendl[c] and Christoph Nowak*[ab]

We demonstrate that double-layered stacks of gold and insulator nanoparticles arranged on a flat gold surface dramatically enhance the sensitivity in absorption infrared microscopy. Through morphological variations of the nanoparticles, the frequency of the plasmon resonances can be tuned to match the frequency of the molecular vibration in the mid-infrared region. The results show that the nanostructures enhance the absorption signal of the molecules by a factor of up to ~2.2 × 10^6, while preserving their characteristic lineshape remarkably well.

The capability to efficiently convert photons into collective oscillations of electrons – plasmons – has led to growing interest in the production and the applications of metallic nanostructures. Plasmons in the visible regime led to the development of new spectroscopic techniques with extreme enhancement of sensitivity, allowing for instance single molecule detection.[1–4] Recently, the fabrication of nanostructures with plasmon excitations in the infrared region has attracted special attention due to their possible application to improve infrared spectroscopic techniques. While most nanostructures for enhanced infrared absorption spectroscopy are arranged on infrared transparent semiconductor platforms,[5–9] we show that a supporting conducting layer can improve plasmon excitations due to the induction of image charges, providing an additional gain in sensitivity.[10,11]

[a]Austrian Institute of Technology GmbH, AIT, Donau-City Str. 1, 1220 Vienna, Austria. E-mail: C.Nowak@ait.ac.at

[b]Center of Electrochemical Surface Technology, CEST, Viktor-Kaplan-Straße 2, 2700 Wiener Neustadt, Austria

[c]Institute of Chemical Technologies and Analytics, Vienna University of Technology, Getreidemarkt 9/164 AC, 1060 Vienna, Austria

[d]Institute for Theoretical Physics, Vienna University of Technology, Wiedner Hauptstraße 8-10/136, A-1040 Vienna, Austria

Generally, infrared absorption spectroscopy is used to investigate vibrational modes associated with specific molecular bonds and chemical functional groups by measuring the absorption in the mid-infrared spectral region.[12] Most significant is the ability to identify conformational changes of proteins that reveal the molecular mechanisms of their functionality.[13–16] The technique is extremely powerful in substance identification, since chemical fingerprints of the most common functional groups can be found in the infrared region and it provides a responsive and almost non-destructive chemical analysis.

Despite such advantages, the moderate sensitivity is one of the major shortcomings that severely limit the application of infrared absorption spectroscopy. Especially in thin samples such as monolayers the absorption signals become prohibitively weak.[17] One way to overcome this fundamental deficit involves leveraging the strong light–matter interaction through enhancing the electromagnetic field in the vicinity of sub-wavelength metallic nanostructures. Enabled by plasmonic resonances in the infrared region, surface enhanced infrared absorption spectroscopy (SEIRAS)[7–9,18,19] was developed in analogy with surface enhanced Raman scattering (SERS)[2,20–22] and surface enhanced fluorescence (SEF).[23–25]

Herein, we demonstrate an enormous gain of sensitivity in infrared absorption spectroscopy using a self-assembled monolayer of dodecanethiol, which shows characteristic symmetric and asymmetric stretching vibrations of the CH_2 and CH_3 groups in the mid-infrared region.[26] Recent studies show that strong enhancement in SEIRAS causes a significant distortion of the molecular signature, which complicates the evaluation of the obtained SEIRAS spectra. These distortions are often called Fano resonances.[6,9,27] Uniquely, our plasmonic system preserves the characteristic shape of the vibrational bands while providing extreme enhancement which enables the monitoring of the absorption signal of a molecular monolayer. Additionally we found that under certain conditions our device can also suppress absorption of molecular vibrations, resulting in so-called window resonances or anti-absorption.[28] Often, theoretical models describe the interaction between molecule

vibrations and plasmons through coupled oscillators, where constructive interference can lead to strong enhancement, but destructive interference can also damp certain vibrations.[27,29,30] We experimentally demonstrate that these effects are related to the relative position of frequencies of the molecular vibration and the plasmon. The scheme in Fig. 1 sums up the morphology of the nanostructure and the interaction between the plasmons and the dodecanethiol monolayer. Our nanostructures represent a transformative advancement in the compatibility of infrared absorption spectroscopy with modern sample preparation. The system allows targeted enhancement of molecular 'fingerprints' with high specificity and additionally can be used to suppress disruptive signals from other molecules within the experiment. In terms of signal enhancement, double-layered nanoparticles provide a consistent evolution of SEIRAS substrates by intensifying their plasmon excitations. For the development of SERS substrates, it was found that insulated metal particles benefit from nearby conducting surfaces, where they can induce image dipole moments.[10,11] This leads to more pronounced plasmon excitations that ultimately increase the enhancement factor. Here, we applied this artifice to design a novel substrate for SEIRAS.

As a first step, we prepared nanoparticle stacks using a lithographic approach and verified their plasmon resonances in the infrared. For this purpose, we prepared glass samples with a stack of continuous layers in the following order: 5 nm adhesive tantalum (Ta), 100 nm gold (Au), 30 nm Ta_2O_5 and 42 nm gold.

The coatings were prepared by direct current magnetron sputtering under an argon atmosphere. The top-down lithographic process used to create the disk-stack nanostructure has been reported previously.[31] The regular arranged disk-stack pattern was defined by electron beam (e-beam) exposure of a negative e-beam resist. After removal of the unexposed parts of the resist, the stack-array structure was created by ion-beam etching. The remaining e-beam resist deposit on top of the disk-stacks was removed by sonication in piranha solution (1 : 3 H_2O_2–H_2SO_4). Further details on this crucial step are provided in the ESI,† due to the fact that clean and resist-free disk-stacks are essential for the formation of self-assembled monolayers.

In order to understand the relationship between the disk-stack diameter and the plasmon resonance frequency, infrared absorption measurements were performed on a dry-air purged infrared microscope (Bruker Hyperion 3000) coupled to a liquid-nitrogen cooled mercury–cadmium telluride detector. IR spectra of each structure were recorded in the spectral region between 8000 and 600 cm^{-1} and calculated as co-addition of 300 scans. The obtained spectra were compared with a simulation model implemented in the MIT Electromagnetic Equation Propagation software package, which utilizes the finite difference time domain (FDTD) method.[32] Further details on the simulations can be found in the ESI.† Fig. 2 shows the absorption spectra of the uncoated disk-stack pattern for various diameters (250–700 nm). The strong absorption signals from the plasmons are in excellent agreement with the FDTD-simulations. The
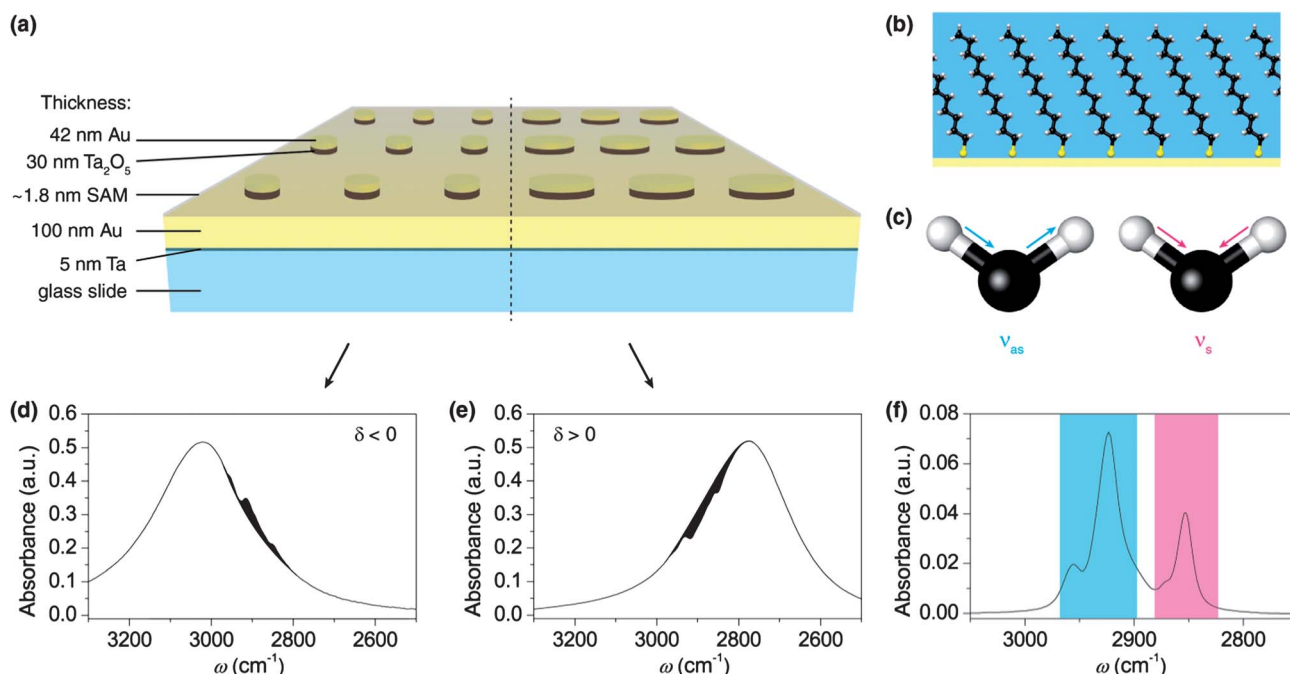

Fig. 1 (a) Scheme of two-dimensional arrays of Ta_2O_5/Au nanoparticles with different stack diameters and a self-assembled monolayer (SAM) of dodecanethiol molecules on the gold surface and on top of the nanoparticles. (b) Graphical representation of the self-assembled monolayer of dodecanethiol on gold. The hydrocarbon chains consisting of CH_2 groups and a CH_3 terminal group form a contact angle of 85° while sulfur is binding to the gold surface. (c) Asymmetric (blue) and symmetric (magenta) stretching modes of CH_2 vibrations. (d) Nanostructures with the plasmon at higher wavenumbers than the molecule vibrations ($\delta < 0$) enhance the molecular absorption. (e) Larger particle diameters (i.e. plasmon at lower wavenumber than the molecule vibration, $\delta > 0$) suppress the molecular vibrations which lowers the total absorbance. (f) ATR-IR absorption spectrum of solute dodecanethiol corresponding to stretching modes depicted in (c).
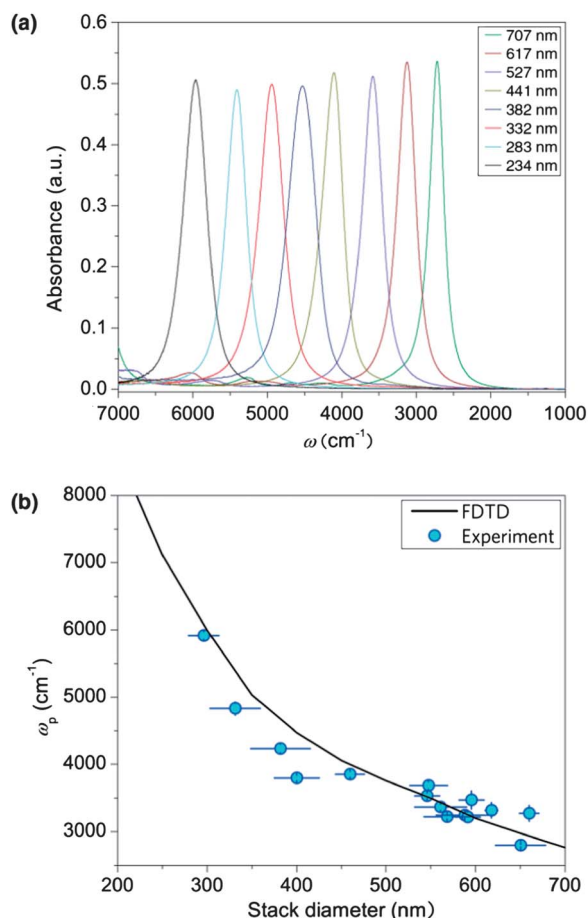
Fig. 2 (a) IR absorption measurements of the double-layered nanoparticles show the tunability of the plasmon resonances by variation of the stack diameters. (b) Blue circles with error bars represent measured resonance positions of the nanostructured device without adsorbed molecules. The black line was calculated for a three dimensional model of the device using finite difference time domain (FDTD) simulations, which are in good agreement with the experimental data.

deviations between the measured resonance positions and the simulation are attributed to fabrication imperfections, which are also analyzed in the ESI† in terms of scanning electron microscopy and focal plane array infrared absorption measurements.

For IR measurements of the monolayer, the diameters of the disk-stacks are adjusted to tune the plasmon resonances in the spectral region of the characteristic band positions of the CH stretching vibrations in the dodecanethiol molecules. The molecular signature of solute dodecanethiol was obtained from attenuated total reflection infrared (ATR-IR) measurements (see Fig. 1f). The spectra are dominated by the methylene (CH_2) group (symmetric stretching vibration ν_s: $\sim$2850 cm^{-1} and asymmetric stretching vibration ν_{as}: $\sim$2925 cm^{-1}).[26] The corresponding absorption of the terminal methyl (CH_3) group is also visible in the spectrum and appears at $\sim$2870 cm^{-1} (ν_s) and $\sim$2960 cm^{-1} (ν_{as}), respectively.

In the next step, the monolayer of dodecanethiol molecules was assembled onto the nanostructures. Therefore, the nanostructured samples were immersed in an ethanolic solution of 1 mM dodecanethiol (98%, Alfa Aeser) for 24 h before rinsing

with pure ethanol and drying with nitrogen gas. The coated substrates were measured with the infrared microscope under the same conditions as the bare structures. Additionally we performed spatially resolved IR microscope measurements within a single grating using a focal plane array (FPA) detector. The spatial resolution helped to monitor the quality of the fabrication and delivered additional information on the enhancement.

The influence of the plasmon position on the enhancement factor was experimentally determined on nanostructures with various diameters. The resulting spectra show that the difference $\delta = \omega_m - \omega_p$ in the spectral position between the plasmon resonance (ω_p) and the molecule-bond vibration (ω_m) crucially influences the enhancement of the absorption signal. Fig. 3 illustrates that the distance parameter δ further determines whether the absorption of the molecular vibration is enhanced or suppressed. For negative values of δ, i.e. when the plasmon resonance is located at higher wavenumbers than the molecule vibration, the characteristic absorption of the molecule is enhanced. For positive values of δ, the effect reverses and the molecular absorbance is suppressed through the plasmon, in analogy to strong damping in coupled oscillator modes for destructive interference.[27,29,30] While the enhancement and suppression depend on the relative position of the frequencies of the molecule vibration and the plasmon, the efficiency of the enhancement or the suppression, related to the coupling strength of the oscillators, depends on the spectral distances between both frequencies. The coupling between plasmon excitation and molecule vibrations already starts at extreme distances. While infrared spectra of the molecular monolayer could not be measured on a flat gold substrate (i.e. when no plasmonic structures are present), nanoparticle-stacks with a plasmonic resonance at a spectral distance of $\sim$1300 cm^{-1} to the molecule vibrations already allowed the detection of their characteristic absorption bands, as shown in the inset of Fig. 3b. To evaluate the coupling strengths for constructive and destructive interferences quantitatively, the band area from this weakly coupled case was used as a reference. Comparing the band area of the asymmetric stretching mode at 2916 cm^{-1} for differently aligned plasmonic resonances to this reference revealed extremely strong growth in the band area.[33] Fig. 3a shows the growth of resonances and window resonances as a function of the spectral displacement between plasmon and molecule resonances. Reducing the distance from 1000 cm^{-1} to 80 cm^{-1} resulted in a maximal signal enhancement of the molecule vibration by a factor of $\sim$125 (Fig. 3c). It is important to stress that this number is not an enhancement factor in the conventional sense, since it is normalized to an already enhanced absorbance signal. To calculate the conventional enhancement factor, we proceeded according to recent literature.[6–9,28] Since the absorption signal of the molecular monolayer on a flat gold surface is below noise level, we performed instead ATR-IR measurements of solute dodecanethiol to obtain the expected value of the normal absorption signal intensity per molecule. Based on the molecule area of $\sim$20 $Å^2$, the monolayer on the disk-stacks contains 1.2×10^{11} molecules, resulting in an absorbance of 0.04 (see Fig. 3b).[34] The number of molecules in
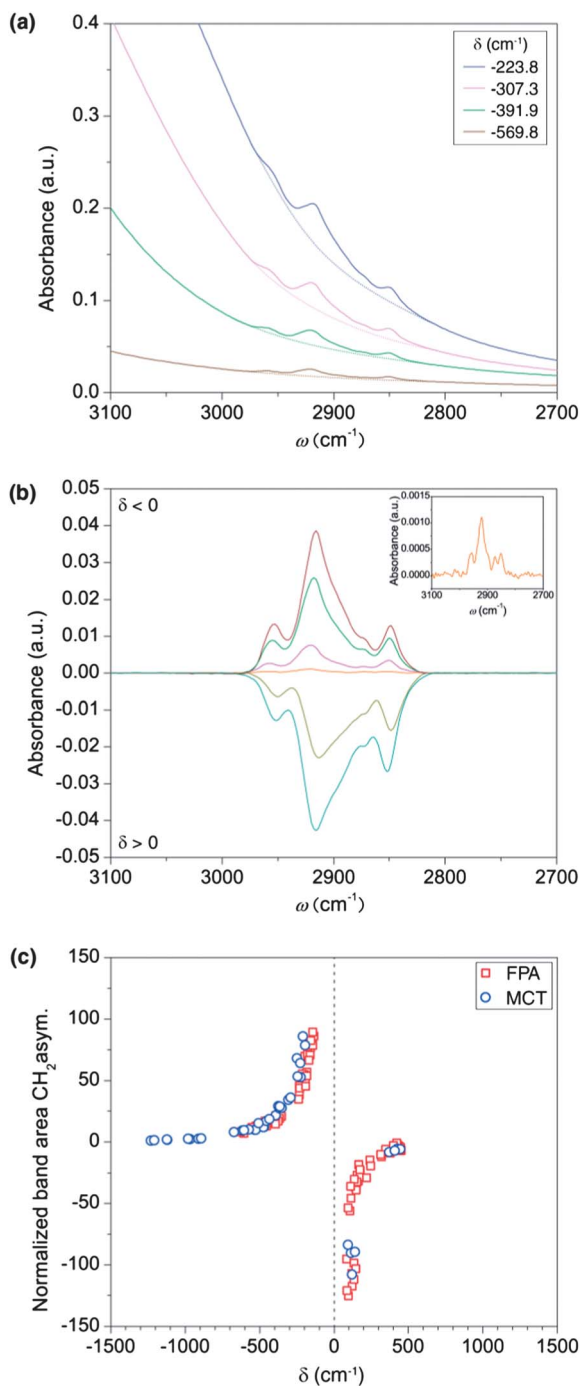
Fig. 3 (a) Infrared absorbance spectra of dodecanethiol monolayers adsorbed onto nanostacks. The intensities of methyl and methylene bands increase for lower δ values, *i.e.* the plasmon resonance is located closer to molecular vibrations. (b) Baseline-corrected IR spectra of C−H vibrations for selected δ values. Negative δ values lead to enhanced absorption, whereas positive δ values form window resonances. The inset shows the enlarged IR-spectrum of the nanostructure with $\delta = -1230$ cm^{-1}, which was the largest distance where a characteristic CH$_2$-band pattern of the monolayer was recognizable. (c) Normalized band areas measured at various spectral distances between plasmon resonance and molecular vibrations. The inset spectrum of (b) was used for normalization to calculate the band area enhancement.

the active area of the evanescent wave in the ATR-IR setup is approximately 1.5×10^{17} molecules, resulting in an absorbance of 0.07 (see Fig. 1f). Considering these amounts of molecules contributing to the absorbance intensities, we estimated the signal enhancement to be $\sim 2.2 \times 10^{6}$. In order to avoid an overestimation of this factor we assumed that all molecules on the nanoparticles contribute to the enhanced signal, even though most published enhancement factors only consider the molecules located at the tips of the nanoantennas.[5-9] Nevertheless, the enhancement is very strong which is mainly attributed to strong coupling between molecule vibrations and the pronounced plasmon excitations. Furthermore, unlike in physisorbed samples a self-assembled monolayer provides transition dipole moments with a fixed orientation to the metal surface, which is beneficial for the sensitivity of the device. A chemisorbed molecule monolayer exhibits a larger enhancement than physisorbed molecules, an effect attributed to the chemical mechanism for surface enhancement.[35] Interestingly, our results in Fig. 3b demonstrate that the shape of the characteristic absorptions of the molecules is approximately preserved for most of the enhancing nanostructures. The distortion of the characteristic signal only becomes relevant for perfectly aligned resonances ($\delta \to 0$). For this case it was not possible to find the correct baseline, which made an evaluation of the enhancement obsolete. For plasmon resonances at a distance greater than ~ 50 cm^{-1}, distortion of the molecule signal reduces dramatically, for both the constructive and the destructive interference. As demonstrated in Fig. 3b, the window resonances in the molecule absorption, resulting from damped molecule vibrations, provide the same quality for monitoring as the enhanced absorption signals, see Fig. 2c.

In summary, we have demonstrated that a metal film supporting the insulated metal particles intensifies infrared plasmon excitations and therefore improves sensitivity. The plasmon resonance position can be tuned by varying the diameter of the disk-stacks, which has a critical influence on the enhancement factor. We successfully demonstrated a strong enhancement of the infrared absorption by detecting a monolayer of dodecanethiol molecules on the nanostructures, while preserving the shape of the characteristic molecular signal. This presents a unique advantage in enhancing sensitivity in infrared absorption spectroscopy using plasmonic structures. Interestingly, we further observed a way to use plasmons to damp specific absorption signals of the molecules, which might be used to suppress disruptive signals from the experimental environment. The practical tunability of the plasmon position for selective signal enhancement poses a versatile platform for the analysis of a wide range of molecular signals.

Acknowledgements

Notes and references

1 B. Fazio, C. D'Andrea, F. Bonaccorso, A. Irrera, G. Calogero, C. Vasi, P. G. Gucciardi, M. Allegrini, A. Toma, D. Chiappe, C. Martella and F. B. de Mongeot, *ACS Nano*, 2011, **5**, 5945–5956.

2 K. Kneipp, Y. Wang, H. Kneipp, L. T. Perelman, I. Itzkan, R. R. Dasari and M. S. Feld, *Phys. Rev. Lett.*, 1997, **78**, 1667–1670.

3 K. M. Mayer, F. Hao, S. Lee, P. Nordlander and J. H. Hafner, *Nanotechnology*, 2010, 21.

4 S. Nie and S. R. Emory, *Science*, 1997, **275**, 1102–1106.

5 R. Adato and H. Altug, *Nat. Commun.*, 2013, **4**, 2154.

6 R. Adato, A. A. Yanik, J. J. Amsden, D. L. Kaplan, F. G. Omenetto, M. K. Hong, S. Erramilli and H. Altug, *Proc. Natl. Acad. Sci. U. S. A.*, 2009, **106**, 19227–19232.

7 C. D'Andrea, J. Bochterle, A. Toma, C. Huck, F. Neubrech, E. Messina, B. Fazio, O. M. Maragò, E. Di Fabrizio, M. Lamy de La Chapelle, P. G. Gucciardi and A. Pucci, *ACS Nano*, 2013, 3522–3531.

8 D. Enders and A. Pucci, *Appl. Phys. Lett.*, 2006, **88**, 184104.

9 F. Neubrech, A. Pucci, T. W. Cornelius, S. Karim, A. Garcia-Etxarri and J. Aizpurua, *Phys. Rev. Lett.*, 2008, **101**, 157403.

10 Y. Chu, M. G. Banaee and K. B. Crozier, *ACS Nano*, 2010, **4**, 2804–2810.

11 Y. Chu and K. B. Crozier, *Opt. Lett.*, 2009, **34**, 244–246.

12 P. Griffiths and J. A. Haseth, *Fourier Transform Infrared Spectrometry*, John Wiley and Sons, 2nd edn, 2007.

13 V. Nedelkovski, A. Schwaighofer, C. A. Wraight, C. Nowak and R. L. C. Naumann, *J. Phys. Chem. C*, 2013, **117**, 16357–16363.

14 C. Nowak, M. G. Santonicola, D. Schach, J. Zhu, R. B. Gennis, S. Ferguson-Miller, D. Baurecht, D. Walz, W. Knoll and R. L. C. Naumann, *Soft Matter*, 2010, **6**, 5523–5532.

15 C. Nowak, D. Schach, J. Gebert, M. Grosserueschkamp, R. B. Gennis, S. Ferguson-Miller, W. Knoll, D. Walz and R. L. C. Naumann, *J. Solid State Electrochem.*, 2011, **15**, 105–114.

16 A. Schwaighofer, S. Ferguson-Miller, R. L. C. Naumann, W. Knoll and C. Nowak, *Appl. Spectrosc.*, 2013, DOI: 10.1366/13-07188.

17 K. Ataka, T. Kottke and J. Heberle, *Angew. Chem., Int. Ed. Engl.*, 2010, **49**, 5416–5424.

18 J. Bochterle, F. Neubrech, T. Nagao and A. Pucci, *ACS Nano*, 2012, **6**, 10917–10923.

19 O. Krauth, G. Fahsold and A. Pucci, *J. Chem. Phys.*, 1999, **110**, 3113–3117.

20 J. A. Creighton, C. G. Blatchford and M. G. Albrecht, *J. Chem. Soc., Faraday Trans. 2*, 1979, **75**, 790–798.

21 M. Fleischmann, P. J. Hendra and A. J. McQuillan, *Chem. Phys. Lett.*, 1974, **26**, 163–166.

22 C. L. Haynes, C. R. Yonzon, X. Y. Zhang and R. P. Van Duyne, *J. Raman Spectrosc.*, 2005, **36**, 471–484.

23 F. Emmanuel and G. Samuel, *J. Phys. D: Appl. Phys.*, 2008, **41**, 013001.

24 P. J. Tarcha, J. Desaja-Gonzalez, S. Rodriguez-Llorente and R. Aroca, *Appl. Spectrosc.*, 1999, **53**, 43–48.

25 J. Zhang, J. Malicka, I. Gryczynski and J. R. Lakowicz, *J. Phys. Chem. B*, 2005, **109**, 7643–7648.

26 B. Stuart, *Biological Applications of Infrared Spectroscopy*, Wiley, New York, 1997.

27 V. Giannini, Y. Francescato, H. Amrania, C. C. Phillips and S. A. Maier, *Nano Lett.*, 2011, **11**, 2835–2840.

28 F. Neubrech and A. Pucci, *IEEE J. Sel. Top. Quantum Electron.*, 2013, **19**, 4600809.

29 R. Adato, A. Artar, S. Erramilli and H. Altug, *Nano Lett.*, 2013, 2584–2591.

30 E. J. Osley, C. G. Biris, P. G. Thompson, R. R. F. Jahromi, P. A. Warburton and N. C. Panoiu, *Phys. Rev. Lett.*, 2013, **110**, 087402.

31 P. Frank, J. Srajer, A. Schwaighofer, A. Kibrom and C. Nowak, *Opt. Lett.*, 2012, **37**, 3603–3605.

32 A. F. Oskooi, D. Roundy, M. Ibanescu, P. Bermel, J. D. Joannopoulos and S. G. Johnson, *Comput. Phys. Commun.*, 2010, **181**, 687–702.

33 A. R. Noble-Luginbuhl and R. G. Nuzzo, *Langmuir*, 2001, **17**, 3937–3944.

34 W. D. Luedtke and U. Landman, *J. Phys. Chem. B*, 1998, **102**, 6566–6572.

35 M. Osawa, in *Near Field Optics and Surface Plasmon Polaritons*, ed. S. Kawata, Springer, Berlin/Heidelberg, 2001, pp. 163–184.